

# Ants (Hymenoptera: Formicidae) from Miocene Ethiopian amber: filling gaps in the geological record of African terrestrial biota

VINCENT PERRICHOT<sup>1,\*</sup>, BRENDON E. BOUDINOT<sup>2,3</sup>, MICHAEL S. ENGEL, FLS<sup>4,5</sup>,  
CHUNPENG XU<sup>6</sup>, BŁAŻEJ BOJARSKI<sup>7</sup> and JACEK SZWEDO<sup>7</sup>

<sup>1</sup>Géosciences Rennes - UMR 6118, Université de Rennes, CNRS 35000 Rennes, France

<sup>2</sup>Institut für Zoologie und Evolutionsforschung, Friedrich-Schiller-Universität Jena, Erberstraße 1, 07743 Jena, Germany

<sup>3</sup>University of California, Davis, One Shields Ave, Davis, California 95616, USA

<sup>4</sup>Division of Entomology, Natural History Museum, and Department of Ecology & Evolutionary Biology, University of Kansas, Lawrence, Kansas 66045, USA

<sup>5</sup>Division of Invertebrate Zoology, American Museum of Natural History, Central Park West at 79<sup>th</sup> Street, New York, New York 10024, USA

<sup>6</sup>State Key Laboratory of Palaeobiology and Stratigraphy, Nanjing Institute of Geology and Palaeontology, Chinese Academy of Sciences, 39 East Beijing Road, Nanjing 210008, China

<sup>7</sup>Laboratory of Evolutionary Entomology and Museum of Amber Inclusions, Department of Invertebrate Zoology and Parasitology, Faculty of Biology, University of Gdansk, 59 Wita Stwosza St., 80-309 Gdansk, Poland

Received 18 January 2022; revised 7 May 2022; accepted for publication 31 May 2022

The Early Miocene (16–23 Mya) amber of Ethiopia constitutes a new source of fossil ants for Africa, where they are otherwise poorly documented. Here we report a diversified assemblage of six subfamilies and at least 19 genera that are still predominantly alive in the Afrotropics today. In this first account, a particular reference is made to the subfamily Dolichoderinae, with the description of two new species: *Technomyrmex svojtkai* Perrichot & Engel **sp. nov.** and *Ravavy goldmani* Boudinot & Perrichot **sp. nov.** The first is illustrated and described based on synchrotron-radiation microcomputed tomography, and the second represents the first fossil record for the tribe Bothriomyrmecini and *Ravavy*, a Malagasy and Afrotropical genus that was hitherto monotypic. The ant composition in Ethiopian amber is congruent with the global pattern emerging across ants and showing a Neogene diversification almost exclusively within extant genera.

**ADDITIONAL KEYWORDS:** Africa – ant diversification – Cenozoic – Dolichoderinae – microtomography – Neogene – *Ravavy* – synchrotron – *Technomyrmex*

## INTRODUCTION

The fossil record of ants (Hymenoptera: Formicidae), although generally extensive, is exceedingly scarce in Africa. To date, only four deposits from the continent have been reported to yield ants, primarily as

compression fossils of incomplete preservation: ten alate specimens representing four species in three genera of uncertain affinity were described from the Late Cretaceous of Botswana (Turonian, c. 91 Mya; [Blussky \*et al.\*, 2004](#); see also: [Archibald \*et al.\*, 2006](#); [LaPolla \*et al.\*, 2013](#)); a petrified colony of *Oecophylla* Smith, 1860 (Formicinae) was described from the Early Miocene of Kenya (16–23 Mya; [Wilson & Taylor, 1964](#)); and a single, undetermined individual was mentioned but not figured from the Middle Eocene of Tanzania (Lutetian, 45 Mya; [Harrison \*et al.\*,](#)

\*Corresponding author. E-mail: [vincent.perrichot@univ-rennes1.fr](mailto:vincent.perrichot@univ-rennes1.fr)

[Version of record, published online 20 July 2022; <http://zoobank.org/urn:lsid:zoobank.org:pub:35706103-4302-459E-A72F-769063E2DB21>]

2001: 62; Schlüter, 2018). Based on a photograph of this specimen kindly provided by Terry Harrison, this latter specimen is assignable to the subfamily Ponerinae (pers. obs., 2014).

Recently, the likelihood for obtaining more substantial material has increased with the discovery of the first African fossiliferous amber in Ethiopia, from which two ants have been reported so far. Ethiopian amber was initially assigned a Cretaceous age (Schmidt *et al.*, 2010), but this notion was soon challenged by the examination of further material (Perrichot *et al.*, 2016, 2018) and the first description of species belonging to extant or derived, post-Cretaceous genera, such as the ant genus *Melissotarsus* Emery, 1877 and the salticid spider †*Gorgopsina* Petrunkevitch, 1955 (Coty *et al.*, 2016; Wunderlich, 2017). Since then, further geological and palynological studies have enabled a revised dating of Ethiopian amber to the Early Miocene (16–23 Mya; see: Bouju & Perrichot, 2020; Bouju, 2021), and taxonomic studies of additional arthropod inclusions have invariably revealed extant genera (Ulitzka, 2020; Bouju *et al.*, 2021, 2022b; Szadziewski *et al.*, 2021; Solórzano-Kraemer *et al.*, 2022).

Apart from the myrmicine *Melissotarsus ethiopiensis* Coty *et al.*, 2016, thus far only one other ant individual of uncertain subfamilial attribution has been reported and figured from Ethiopian amber (Schmidt *et al.*, 2010: fig. 3A). This ant fossil was later identified as a member of Dolichoderinae (LaPolla *et al.*, 2013: suppl. fig. 5). Here we formally describe this fossil and further subsequently discovered dolichoderines from Ethiopian amber, comprising one new species each in the extant genera *Technomyrmex* Mayr, 1872 and *Ravavy* Fisher, 2009. We also provide an overview of the ant diversity in Ethiopian amber, including an inventory of other subfamilies and genera identified from four institutional collections, of which a detailed taxonomic treatment will be proposed in future studies.

## MATERIAL AND METHODS

### AMBER SPECIMENS

The studied specimens are contained in four amber pieces housed in the following public repositories: Nanjing Institute of Geology and Palaeontology (NIGPAS, China), the Geological Museum of the University of Rennes (IGR, France), the Museum of Amber Inclusions of the University of Gdansk (MAIG, Poland) and the Natural History Museum of Vienna (NHMW, Austria). The fossils originated from various deposits of the North Shewa and South Wollo Zones of the Amhara region (for details on the localities, refer to: Bouju *et al.*, 2021, 2022a). Ethiopian amber is

generally collected from siltstone exposed in gorges of rivers incising the north-western Ethiopian Plateau. Analyses of the palynomorphs from the amber-bearing siltstone indicate an Early Miocene age for all these deposits.

Specimen NHMW-N6976 was part of the sample surveyed by Schmidt *et al.* (2010) and originates from a deposit near Alem Ketema, in the North Shewa Zone. While the ant is preserved in a piece of translucent amber, its detailed examination was made particularly difficult owing to its position of preservation, i.e. with legs and antennae retracted along the curled body so that the face, mesosoma, petiole and apex of the gaster are rendered mostly invisible (Fig. 1A). Therefore, the specimen was imaged using X-ray synchrotron microtomography and the different structures visualized after a virtual dissection (see below for details on the imaging technique).

Specimen MAIG 6020 comes from a deposit near the town of Weldiya in the south-east of the South Wollo Zone (see details about this deposit in: Bouju *et al.*, 2021). The amber piece contains diverse remains of cryptogams and insects, including four dolichoderine ant workers missing various body parts such as the head, gaster or legs.

Specimens NIGP180512 and IGR.ET2015/001a were purchased from a gem trader in Addis Ababa and come from one of the four deposits of the North Shewa Zone mentioned by Bouju *et al.* (2022a: fig. 2), although the exact locality is unknown. Both amber pieces originally contained one male dolichoderine together with various myrmicine ants and other arthropod or plant inclusions. These pieces were cut into six and two fragments, respectively, and each fragment was ground and polished from all sides in order to enhance the visibility of inclusions and facilitate their study and photography. All amber pieces were legally purchased from a licensed gemstone trader in Addis Ababa, and export permits obtained from the Ethiopian Ministry of Mines and Petroleum.

### EXAMINATION AND IMAGING

The specimens were examined, measured and photographed using various optical stereomicroscopes equipped with a digital camera. For best photographic results, a drop of water was applied to the amber surface above the region of interest and covered with a glass coverslip (for recommendations on the preparation and imaging of amber inclusions, see: Sadowski *et al.*, 2021). All images are digitally stacked composites of multiple focal planes, and most were obtained using HELICON FOCUS software, with the exception of the two specimens of *Ravavy*. The latter were imaged with a Canon EOS 7D equipped

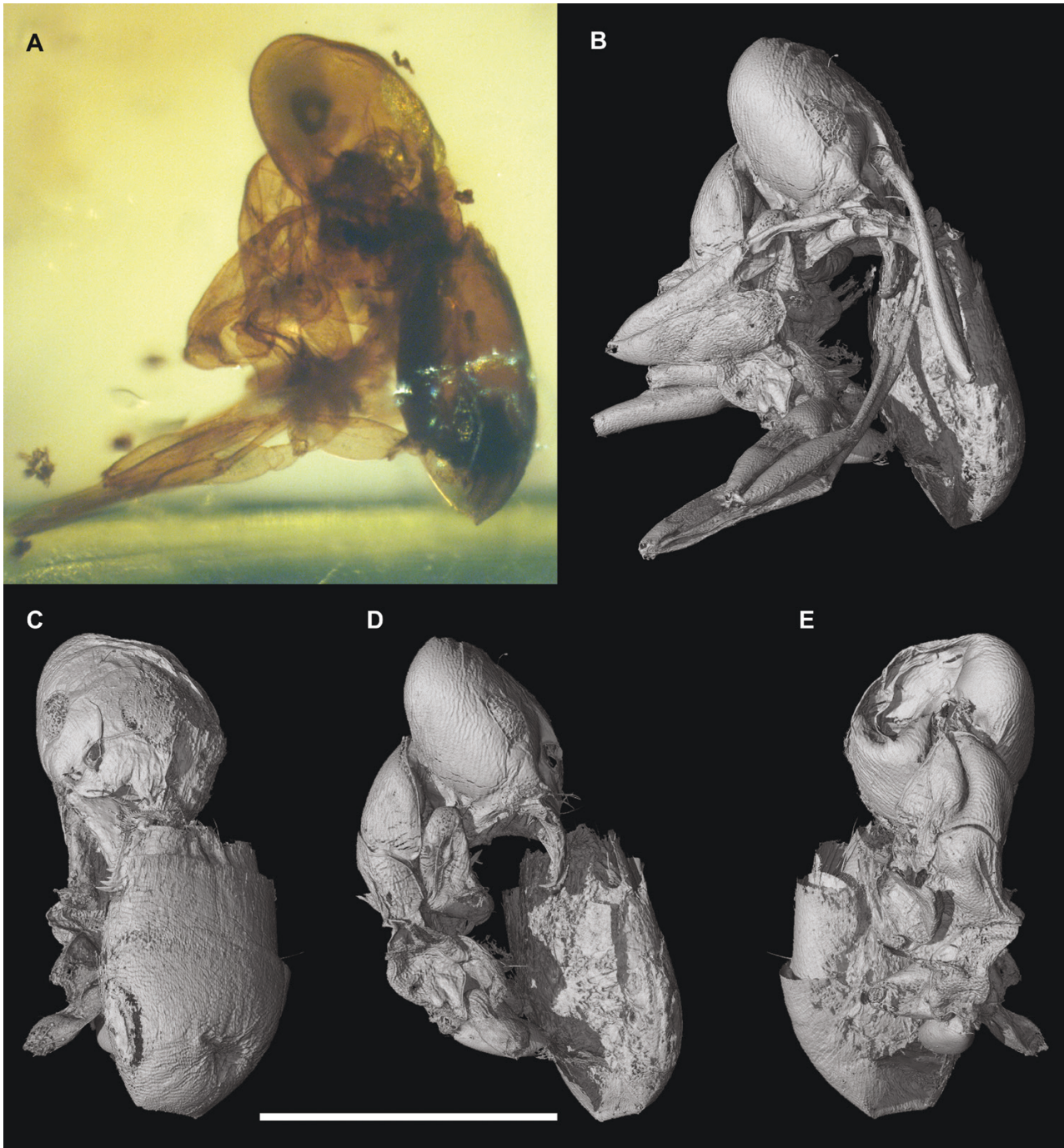


**Figure 1.** *Technomyrmex svojtkai* sp. nov., holotype worker NHMW-N6976. A, photomicrograph in right lateral view, with tip of gaster curled toward the mouthparts. B, 3D model in nearly the same position, imaged by synchrotron microtomography. C–E, 3D model of body with antennae and legs virtually removed: C, anterior (frontal) view; D, left lateral view; E, posterior (dorsal) view. Scale bar: 0.5 mm. Animated versions of this are available in Supporting Information online ([Figs S1, S2](#)).

with a Canon MP-E 65 mm macro lens, with the camera attached to a StackShot rail (Cognisys Inc.); lighting was provided by a pair of synchronized YN560 Speedlite (Yongnuo Photographic Equipment Co.) flashes; stacks were then exported as tiffs using

ADOBE LIGHTROOM and montaged using ZERENE STACKER (Zerene Systems LLC). All figures were composed with ADOBE PHOTOSHOP.

The specimen NHMW-N6976 was imaged at the European Synchrotron Radiation Facility (ESRF,



Grenoble) using a propagation phase-contrast X-ray microtomography protocol described in detail by [Lak et al. \(2008\)](#). The amber piece was scanned using a monochromatic beam with an acceleration voltage of 17 keV, an isotropic voxel size of 0.678 µm and a propagation distance of 145 mm between the sample and the detector. The tomography consisted of 1500 projections acquired through a 180° rotation and 0.5 s of exposure time. After the acquisition, the volume was reconstructed using filtered back-projection algorithms adapted for local tomography applications (PyHST, ESRF), and later segmented using a manual region growing protocol in VGSTUDIOMAX 3.0 software (Volume Graphics, Germany). Virtual dissections were made using the same software.

#### MORPHOLOGICAL TERMINOLOGY

Terminology for the head follows [Richter et al. \(2020\)](#); the head is described as if it were prognathous for both the worker and male. Mesosomal terms for the worker follow [Bolton \(1994, 2007\)](#) and [Keller \(2011\)](#), while alate-specific terms, including wing venation, follow [Boudinot \(2015\)](#). Genitalic terminology follows [Boudinot \(2013, 2018\)](#); the following terms are favoured from the latter work: gonopods (= ‘parameres’), gonocoxite (= ‘basimere’), gonostylus (= ‘telomere’) and penite (= penisvalva). ‘Imbricate’ is used in the sense of [Harris \(1979\)](#) for sculpture, i.e. with an even pattern of polygonal scutes that demarcate the underlying epithelial cell margins ([Mikó et al., 2016](#)).

#### MEASUREMENTS AND INDICES

Measurements (all in mm) and indices follow [Bolton’s \(2007\)](#) revision of *Technomyrmex*. Specimens were measured from photographs in ADOBE ILLUSTRATOR CC 2019, or from 3D reconstruction in VGSTUDIOMAX 3.4; measurement files and values for males of the *Ravavy* species are provided in the [Supporting Information, Appendix S1](#). Except male-specific variables indicated by an asterisk (\*), the main metrics can be visualized in [Figure 2](#):

BL Body length: the total body length from the anterior margin of the head excluding mandibles to the apex of the abdomen, measured in dorsal view.

HL Head length: the length of the head capsule excluding the mandibles; measured in full-face view in a straight line from a line that spans the anteriormost points of the clypeal lobes to the level of a line that spans the posterior corners of the head capsule.

HW Head width: the maximum width of the head immediately behind the eyes, measured in full-face view.

HWE\* Head width, eyes: the maximum width of the head, including the compound eyes.

SL Scape length: the maximum straight-line length of the scape, excluding the basal constriction or neck that occurs just distad of the condylar bulb.

FcW Frontal carinae width: the distance across the separation of the frontal carinae at torular mid-level, measured in full-face view.

EL Eye length: in profile, the maximum measurable length of the compound eye.

OLL\* Ocellus length, lateral: the maximum length of the lateral ocellus, measured in full-face view.

OIL\* Inter-ocellus length: the minimum distance between the lateral ocelli, measured in full-face view.

WL Weber’s length: the diagonal length of the mesosoma in profile, from the angle at which the pronotum meets the cervix to the posterior basal angle of the metapleuron.

ML\* Mesoscutum length: the maximum length of the mesoscutum, measured in dorsal view.

MW\* Mesoscutum width: the maximum width of the mesoscutum, measured in dorsal view.

FWL\* Forewing length: the maximum length of the forewing from the apices of the axillary sclerites to the wing apex.

PH Petiole height: the maximum height of petiole (abdominal segment 2), measured in profile view.

PL Petiole length: the maximum length of petiole (abdominal segment 2), measured in dorsal view.

PW Petiole width: the maximum width of petiole (abdominal segment 2), measured in dorsal view.

GL Gaster length: the maximum length of gaster (abdominal tergites 3 to 7), measured in dorsal view.

GW Gaster width: the maximum width of gaster, measured in dorsal view.

CI Cephalic index:  $HW/HL \times 100$ .

HWI\* Head width index:  $HW/HWE \times 100$ .

SIS Scape index:  $SL/HW \times 100$ .

OI Ocular index:  $EL/HL \times 100$ .

OCI\* Ocellar index:  $OLL/OIL \times 100$ .

EPI Eye position index: in full-face view, the distance from a horizontal line that spans the anterior clypeal margin to one that spans the anterior margins of the eyes, divided by the distance from a horizontal line that spans the posterior margins of the eyes to one that spans the posterior corners of the head,  $\times 100$ .

MI\* Mesoscutum index:  $MW/ML \times 100$ .

PI\* Petiolar index:  $PL/PH \times 100$ .

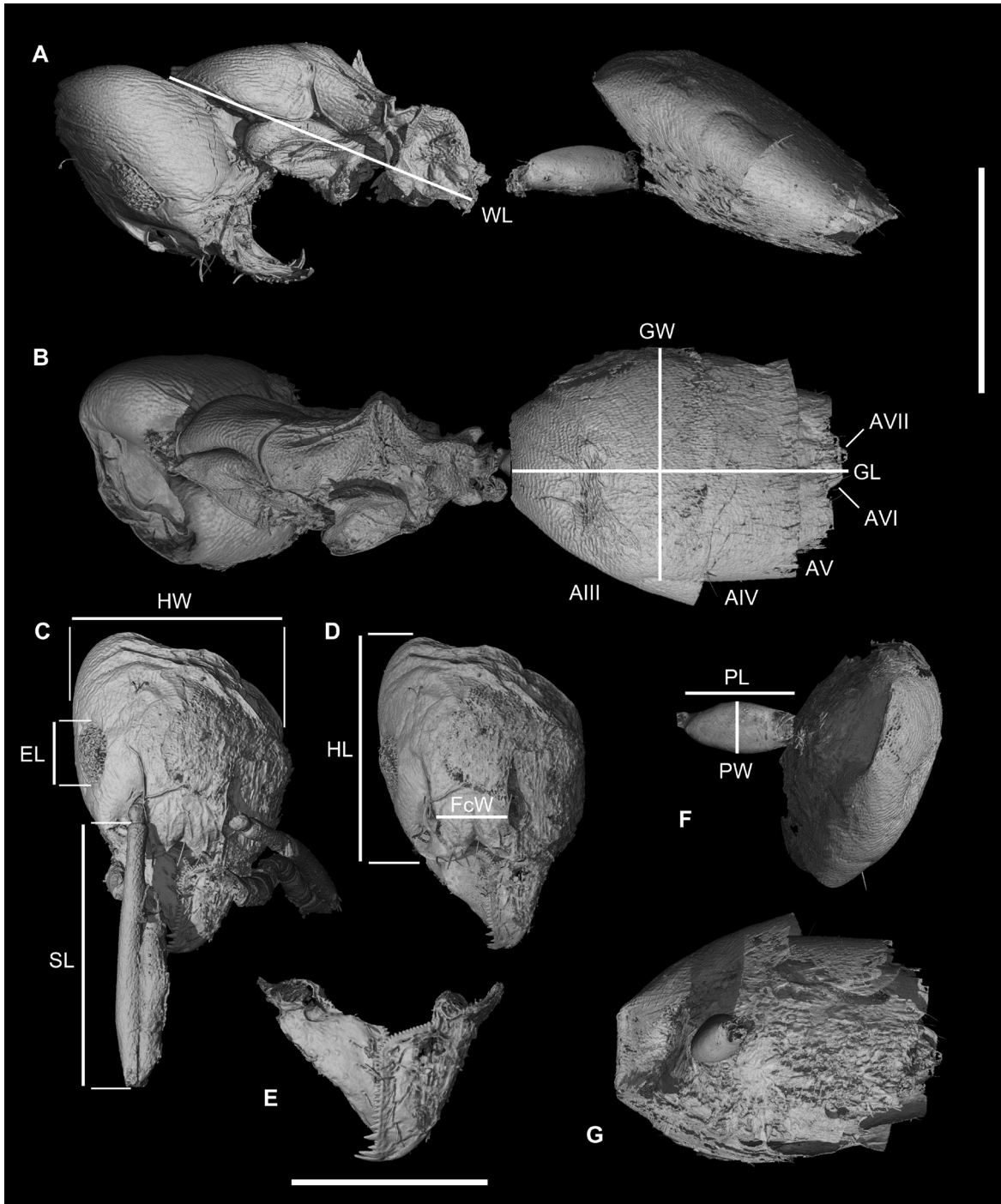


**Figure 2.** *Technomyrmex svojtkai* sp. nov. Phase contrast X-ray synchrotron microtomography of holotype worker NHMW-N6976, with indication of measurements as reported in Material and methods. A, lateral view of body with legs and antennae virtually removed, and with petiole and gaster virtually uncurled to approximate the life position. The left lateral side of the head and mesosoma being crushed, the figure shows them from the horizontally flipped right side in standard left profile view. B, reconstruction in dorsal view, without legs and antennae, and with gaster largely concealing the petiole as in approximate life position. C, head in full-face view. D, head without antennae in full-face view. E, mandibles in dorsal view. F, petiole in dorsal view, with articulation with gaster as preserved. G, gaster in ventral view, with articulation with petiole as preserved, showing the first gastral tergite concavity for accommodation of petiole. Abbreviations: AIII–AVII, abdominal segments III to VII. Scale bars: 0.5 mm, except 0.2 mm for E.

## RESULTS

## SYSTEMATIC PALAEOONTOLOGY

FAMILY FORMICIDAE LATREILLE, 1809

SUBFAMILY DOLICHODERINAE FOREL, 1878

TRIBE TAPINOMINI EMERY, 1913

GENUS *TECHNOMYRMEX* MAYR, 1872

*Type species: Technomyrmex strenuus* Mayr, 1872: 147.

***TECHNOMYRMEX SVOJTKAI* PERRICHOT & ENGEL  
SP. NOV.**

(FIGS 1–3; SUPPORTING INFORMATION, FIGS S1, S2)

*Zoobank registration:* urn:lsid:zoobank.org:act:565B4980-A80E-450B-A09B-603264A91F50.

*Type material:* Holotype NHMW-N6976, a complete worker; in Early Miocene (16–23 Mya) amber from the

North Shewa Zone, Amhara region, Ethiopia; housed in the Department of Mineralogy and Petrography, Naturhistorisches Museum Wien (NHMW, Austria). Paratypes MAIG 6020, two workers missing portions of legs; in Early Miocene (16–23 Mya) amber from the South Wollo Zone, Amhara region, Ethiopia; housed in the Museum of Amber Inclusions of the University of Gdansk (MAIG, Poland).

*Other material:* MAIG 6020, one worker missing the head, portions of legs and gaster, but similar to the associated paratypes in its size and preserved structures, particularly the subcylindrical petiole, the shape and position of metathoracic and propodeal spiracles, thus considered here as conspecific; housed in the Museum of Amber Inclusions of the University of Gdansk (MAIG, Poland).

*Etymology:* The specific epithet honours Mr Matthias Svojtka (University of Vienna) who discovered the

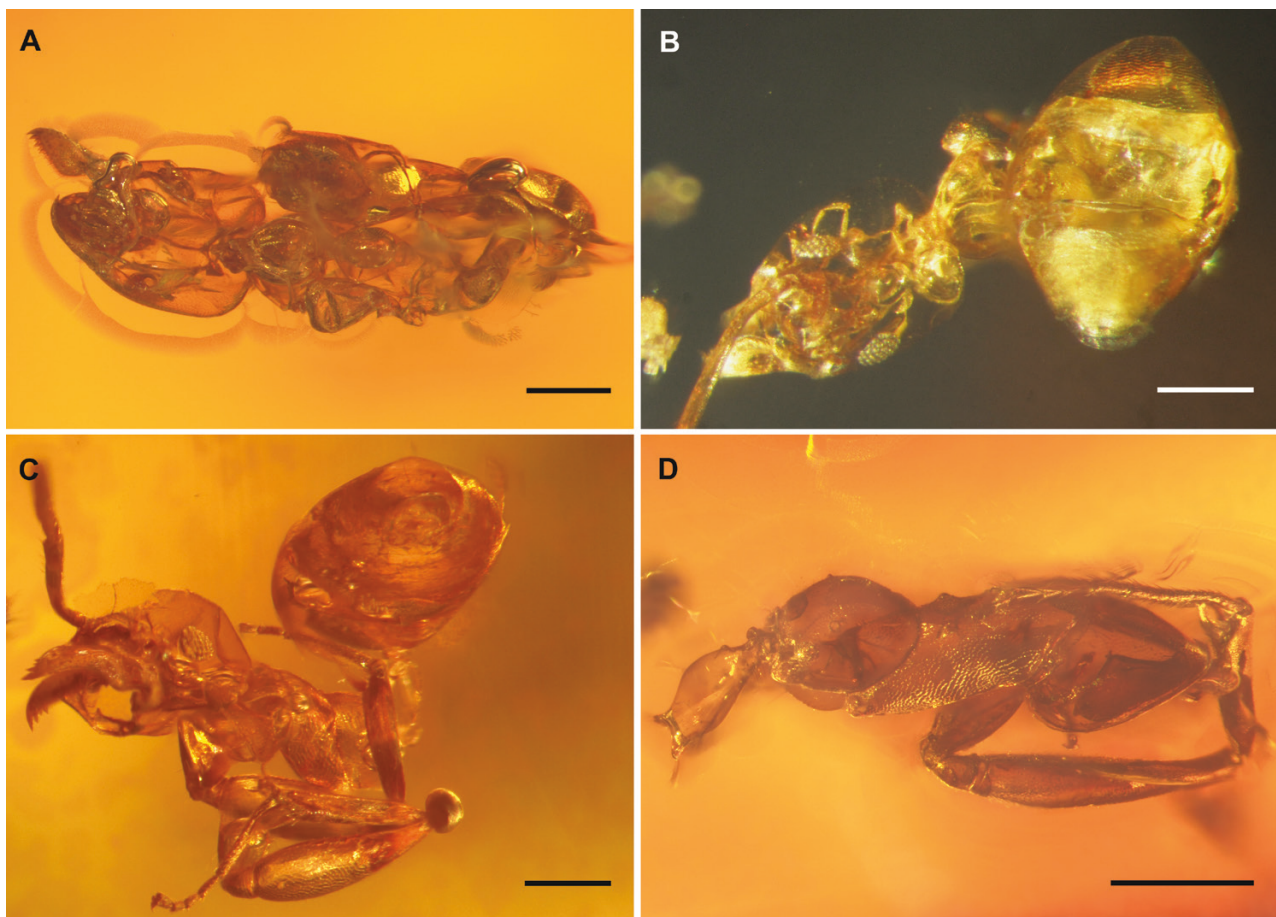


**Figure 3.** *Technomyrmex svojtkai* sp. nov., photomicrographs of paratype workers and additional, partial worker, specimen MAIG 6020. A, paratype 1, ventral view. B, paratype 2, dorsal view. C, paratype 2, left lateral view, anterior-oblique orientation. D, non-type, partially preserved worker, right lateral view. Scale bars: 0.25 mm.



fossil representing the holotype and generously made it available for study.

**Diagnosis:** The species is uniquely identified within *Technomyrmex* by the following combination of worker characters: (1) anterior clypeal margin with a deep V-shaped median incision; (2) inner margins of incision continuously arched, with no marked angle with broadly semicircular anterolateral clypeal margins; (3) dorsum of head with a single pair of stiff setae situated above posterior level of eyes; (4) compound eyes situated around midlength of head (EPI 59), with about 40 ommatidia; (5) palp formula 6,4; (6) mandible with six conspicuous teeth apically on masticatory margin; (7) counting from the apex, first tooth longest, third and fifth teeth subequal in length, smaller than second and fourth, third to sixth teeth each separated by one denticle, sixth tooth followed by a continuous series of smaller teeth gradually decreasing in size along masticatory margin and basal angle, becoming denticles along entire basal margin; (8) the basal angle indistinct, continuously arched between margins; (9) mesosoma devoid of erect setae; (10) propodeal dorsum as long as declivitous face, their junction broadly rounded.

**Description:** Holotype. Body integument minutely asperous, mostly glabrous except sparse stiff setae on anterior head margin and gaster. Head only slightly longer than wide. Compound eye oval, moderately large and feebly convex, its outer margin barely surpassing the outline of sides in full-face view, with 38–40 ommatidia. Ocelli absent. Frontal carinae well distant, closer to inner margin of eyes than to each other, not surpassing posterior margin of eyes and without frontal lobe, such that antennal sockets entirely exposed although directed laterad. Antenna 12-merous, scape surpassing vertexal margin by more than one-third its length; first and terminal funicular antennomeres subequal in length, nearly twice as long as broad; all other antennomeres cylindrical, only slightly longer than broad. Vertex with an erect seta (likely paired, but upper left side of head altered) longitudinally aligned with frontal carina, in profile situated at midlength between posterior margins of eye and head. Anterior clypeal margin bordered by seven stiff, short setae inclined ventrally; posterior clypeal margin semicircular, even with posterior level of toruli. Mesosoma: in profile, mesonotal dorsal outline feebly convex in its anterior third, flat and sloped in its posterior two thirds. Mesonotum and propodeum forming a distinct angle at metanotal groove. Metathoracic spiracles raised into distinct tubercles, conspicuously breaking outline of mesosoma in lateral view, distinctly anterior to

metanotal groove. Dorsal surface of propodeum flat, declivitous surface convex. In profile, propodeal spiracle at junction of lateral and declivitous surfaces, slightly above midheight of sclerite. Dorsal surface of mesosoma apparently without erect setae. Legs: mesotibia and metatibia each with one spur, that of metatibia pectinate. Metasoma: petiole more than twice as long as wide, nearly as wide as high, broadest around its midlength; ventral and dorsal surfaces feebly convex; ventral surface without lobe, with two anterior longitudinal rows of three short setae. Gaster: abdominal tergite III largest, ventral surface of its anterior projection with a groove that accommodates entire petiole. Tergites III–VI with posterior margin bordered by a row of short appressed setae barely surpassing margin. Tergite VII in dorsal view small, trapezoidal.

**Paratypes and other specimens:** As for the holotype, although incomplete or partially concealed due to preservation, but with posterior margin of head intact, not emarginate (MAIG 6020 paratypes); palpomeres clearly exposed (MAIG 6020 paratype 1), revealing a palp formula 6,4, with maxillary palp relatively long, exceeding hypostomal margin but not reaching occiput, and labial palp short, about one-third length of maxillary palp; mesonotum constricted and elongate (MAIG 6020 additional worker).

**Measurements and indices:** Abbreviations are explained in Material and methods. Holotype: BL ~ 2.00, HL 0.50, HW 0.49, EL 0.15, FcW 0.18, SL 0.59, WL 0.77, PL 0.30, PW 0.13, PH 0.12, GL 0.80, GW 0.55, CI 98, OI 30, EPI 59, SI 129. Paratypes and additional worker: HL 0.52–0.54, HW 0.46, EL 0.11–0.15, SL 0.52, WL 0.77, PL 0.25–0.35, PW 0.20, SI 110.

**Note:** Amber piece MAIG 6020 also contains a fourth, partially preserved worker, which displays a similar petiole and can probably be attributed to *Technomyrmex*. However, only the mesosoma and petiole are preserved, and it differs by a larger size (WL ~ 2.40 vs. 0.77; PL 0.77 vs. 0.25–0.35) and the presence of a dense, short pubescence covering all sclerites; it probably belongs to another species.

Among the dolichoderines, the petiole reduced to a low segment without a node or scale and overhung by the first gastral segment, which is anteriorly grooved, is shared by *Technomyrmex* and *Tapinoma* Förster, 1850. The pygidium exposed in dorsal view, thus with five gastral tergites visible, as is seen on the new fossil, warrants placement in *Technomyrmex* (whereas the pygidium is reflexed ventrally, exposing only four gastral tergites in dorsal view in *Tapinoma*; see, e.g. Bolton, 2007; Fisher & Bolton, 2016).

The new species is readily recognizable by its anterior clypeal margin with a deep V-shaped incision and broadly rounded lateral margins, the almost complete lack of erect setae on the dorsum of head, mesosoma and first gastral tergite (with the exception of a single pair of setae posterior to the frontal carinae), and the propodeal dorsum that is as long as, or even slightly longer than, the declivitous surface. In all other species of *Technomyrmex* with a deeply incised clypeal margin, the median notch is either U-shaped or semicircular, but never V-shaped. These and other features, such as the elongate mesosoma and metathoracic spiracles raised on tubercles, suggest that *Technomyrmex svojtkai* may belong to the *bicolor* group of species as defined by Bolton (2007).

TRIBE BOTHRIOMYRMECINI DUBOVIKOFF, 2005

GENUS *RAVAVY* FISHER, 2009

*Type species:* *Ravavy miafina* Fisher, 2009: 47, figs 6, 7b.

***RAVAVY GOLDMANI* BOUDINOT & PERRICHOT  
SP. NOV.**

(FIGS 4–5)

*Zoobank registration:* urn:lsid:zoobank.org:act:693FB2F0-817E-4BD6-B2E4-5585AFC99EA2.

*Type material:* Holotype NIGP180512, male, housed in the Nanjing Institute of Geology and Palaeontology (NIGPAS, China); paratype IGR.ET2015/001a, male,



**Figure 4.** *Ravavy goldmani* sp. nov., holotype male NIGP180512, photomicrographs. A, left lateral view, slightly anterior-oblique orientation. B, ventral view, slightly left-lateral-oblique orientation. Scale bars: 0.5 mm.



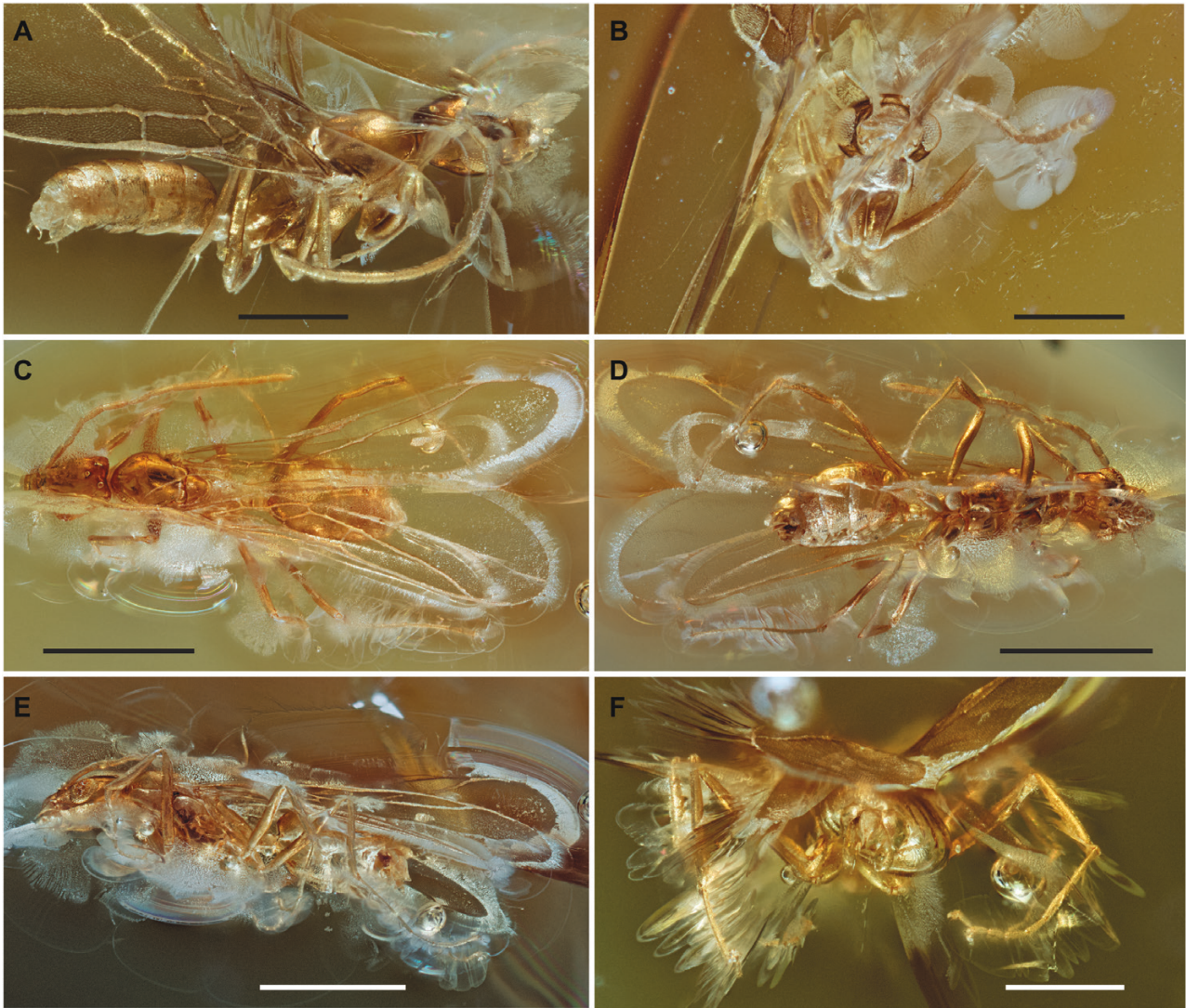


**Figure 5.** *Ravavy goldmani* sp. nov., photomicrographs. A–B, holotype male NIGP180512, C–F, paratype male IGR. ET2015/001a. A, right lateral view, slightly posterodorsal–oblique orientation. B, oral view, slightly right–lateral–oblique orientation. C, dorsal view, slightly right lateral, anterior oblique orientation. D, ventral view, slightly right–lateral, posterior oblique orientation. E, right lateral, slightly ventral, anterior oblique view. F, caudal view of genitalia, slightly right lateral oblique. Scale bars: 0.5 mm for A, B, F; 1.0 mm for C–E.

housed in the Geological Museum of the University of Rennes (IGR, France). In Early Miocene (16–23 Mya) amber from the North Shewa Zone, Amhara region, Ethiopia.

**Etymology:** The specific epithet honours Mr Yale Goldman (Bloomfield, Connecticut) who kindly facilitated access to the type specimens of the new species.

**Diagnosis:** Because of the limited knowledge of male ants at the global scale, this diagnosis is broken into

four parts in order to establish the identity of the treated specimens: identification at the subfamilial, tribal, generic and species levels.

(I) Identifiable as Dolichoderinae by the following combination: (1) clypeal condyle large, rhomboidal (see note 1 below); (2) forewing cross-vein cu-a prefurcal, i.e. joining M+Cu proximad branching point of M and Cu; (3) helcium infraaxial; (4) abdominal segment III unpetiolated, i.e. not reduced in size relative to segment IV; (5) prora absent; (6) abdominal segment IV without cinctus; (7) gonostylus dorsoventrally short relative to

gonocoxite, proximally constricted and not extending proximad gonocoxite (note 2); (8) basivolsellar process present (note 3).

(II) Identifiable as Bothriomyrmecini by the following combination (note 4): (9) clypeus not extending posteriorly between toruli; (10) medial hypostomal lamina absent; (11) forewing cross-vein 2rs-m absent.

(III) Identifiable as *Ravavy* by the following features, all of which are unique within Bothriomyrmecini (note 5): (12) mandible unidentate, spatulate with an apical spiniform tooth (vs. mandible multidentate, strap-shaped to spiniform) (note 6); (13) palp formula 6,3 (vs. 6,4 or  $\leq 4,3$ ) (note 7); (14) pterostigma situated immediately proximad forewing midlength (vs. situated distad); (15) marginal cell extremely long, somewhat more than twice the length of submarginal cell 1; (16) Rf appendix, i.e. distalmost free abscissa of R, long, somewhat shorter than pterostigma; (17) discal cell subrectangular, longer proximodistally than wide anteroposteriorly and size small; (18) petiolar node broadly convex in profile view (vs. anteroposteriorly narrow and squamiform); (19) penite apices not downcurved, but rather being produced distally as long, linear processes.

(IV) Distinguished from *Ravavy miafina* by the following (note 8): (20) smaller, BL  $\sim 2.57$ – $2.34$ , WL  $\sim 0.43$ – $0.46$ , FWL  $\sim 2.17$ – $2.52$  (vs. larger, BL  $\sim 3.33$ – $4.46$ , WL  $\sim 1.30$ – $1.67$ , FWL  $\sim 3.85$ – $3.99$ ); (21) head somewhat broader, CI  $\sim 122$  (vs. narrower, CI  $\sim 112$ – $114$ , although 122 in one specimen); (22) malar space relatively long, MSI  $\sim 6$  and space distinctly longer than proximal width of mandible in lateral view (vs. relatively short, MSI  $\sim 28$ – $32$  and distinctly shorter than proximal mandibular width); (23) eye relatively long, OI  $\sim 40$ – $39$  (vs. eye relatively short, OI  $\sim 14$ – $18$ ); (24) ocelli relatively small, OCI  $\sim 38$  (vs.  $44$ – $62$ ); (25) antennomere III but not IV slightly kinked (vs. both antennomeres kinked); (26) mesoscutum relatively long, MI  $\sim 80$  (vs. short, MI  $\sim 104$ – $131$ ); (27) scutoscuteellar sulcus distinctly broad (vs. short, almost line-like); (28) petiole relatively long, PI  $\sim 80$  (vs. short, PI  $\sim 51$ – $67$ ); (29) bristle-like setae apparently not developed on gastral sternites (vs. such setae present on all gastral sternites except the first); (30) abdominal sternum IX posterior margin broadly convex (vs. broadly emarginate); (31) gonostyli relatively long, length  $\sim 2$ – $3 \times$  height (vs. short, length  $\sim 1 \times$  height); (32) gonostylar apices narrowly pointed (vs. broadly rounded); (33) ventral margin of penite more-or-less linear from base to apex (vs. base produced ventrally as a dorsoventrally long, anteroposteriorly narrow, serrate lobe); and (34) apicoventral penite processes short, length from proximodorsal inflection point  $\sim 1 \times$  height (vs. long, length  $\sim 4 \times$  height).

Notes on diagnosis:

1. A large, rhomboidal clypeal condyle is an apparent synapomorphy of the Dolichoderomorpha, i.e. Dolichoderinae + Aneuretinae. The clypeal condyle of Formicinae and other subfamilies is variable in shape, often anteroposteriorly narrow.
2. The form of the gonopod is an apparent synapomorphy of Dolichoderinae as it is not shared with Aneuretinae.
3. Most dolichoderines have a posteroventral (ventroapical) basivolsellar process, which may be short and triangular to elongate and digitate. The process is absent in *Azteca* Forel, 1878 and *Gracilidris* Wild & Cuzzo, 2006 (sister taxa), *Ochetellus* Shattuck, 1992 and some *Dolichoderus* Lund, 1831. Formicines do not have a basivolsellar process; such a process is present convergently in the Amblyoponinae, which is a synapomorphy for that subfamily (Yoshimura & Fisher, 2012; Boudinot, 2015).
4. In their recent phylogenetic revision of the Dolichoderinae, Ward *et al.* (2010) provided reduction or loss of the medial hypostomal lamina as a synapomorphy of the Bothriomyrmecini that occurs in both sexes. Subsequently, Boudinot *et al.* (2016) recognized loss of forewing cross-vein 2rs-m as another diagnostic condition. Here, we propose the ‘short’ condition of the clypeus as an additional synapomorphy of the tribe. The clypeus in both males and females extends posteriorly between the antennal toruli in the majority of dolichoderine genera with only a few exceptions (Shattuck, 1992; Boudinot, 2015), such as the *neotropicus* and *macro* clades of *Leptomyrmex* Mayr, 1862 (Lucky & Ward, 2010; Boudinot *et al.*, 2016; Barden *et al.*, 2017).
5. Males and queens of the Bornean genus *Loweriella* Shattuck, 1992 are unknown in contrast to the other three bothriomyrmecine genera (*Bothriomyrmex* Emery, 1869a, *Chronoxenus* Santschi, 1919, *Ravavy*). Because *Loweriella* is the sister-group of *Ravavy* (Ward *et al.*, 2010), a number of the diagnostic traits of the latter genus adduced here may be synapomorphies of the two genera.
6. Yoshimura & Fisher (2011) tentatively remarked that additional, vestigial denticles may be present in *R. miafina* and label a possible denticle on a dissected mandible imaged with a compound microscope. Because this apparent denticle is on the lateral mandibular margin, and as the apical tooth is a consistent feature of even ‘edentate’ mandibles (Boudinot *et al.*, 2021), we interpret the mandible of *R. miafina* as strictly unidentate.
7. The 6,3 palpomere count is an apparent synapomorphy of *Ravavy* within the Bothriomyrmecini. *Loweriella* has a plesiomorphic 6,4 count, while



*Bothriomyrmex* and *Chronoxenus* share a derived, reduced count which is  $\leq 4,3$  (Bolton, 2003; Fisher, 2009; Yoshimura & Fisher, 2011).

8. The fine anatomy and morphology of *R. miafina* is illustrated in Fisher (2009) and especially Yoshimura & Fisher (2011). The latter work provided a revised diagnosis of this species plus a comparative analysis of genitalic form. Comparisons were made to the images in the literature, on AntWeb (2022), and to specimens examined at the California Academy of Sciences.

**Description:** Integument uniformly imbricate, apparently with a more-or-less even vestiture of extremely short and appressed pubescence; bristle-like setae not visible on body with exception of tarsi, gastral tergites and gonostyli, those of gastral tergites sparse. Head roughly rectangular, narrow anterad eyes and broader posteriorly; malar space relatively broad, being longer than proximal width of mandible in lateral view; posterior head margin emarginate. Compound eye bulging, length slightly less than half head-length, subreniform with subtle emargination occurring on along ventral eye margin and with > 175 ommatidia but probably not more than 200 (complete count not possible). Ocelli small; lateral ocelli relatively wideset, separated from one another by somewhat more than three lateral ocellar lengths. Frontal carinae poorly developed. Antenna 13-merous, scape about as long as compound eye and about 3 × as long as pedicel; pedicel about twice as long as wide and slightly more than half the length of antennomere III; antennomere III slightly kinked at about midlength; antennomeres III–XIII subequal in length and about 4 × as long as wide. Ocellar sensilla (setae) not visible. Anterior clypeal margin more-or-less linear; clypeal setation not observable; posterior clypeal margin convex, portion of epistomal sulcus anterad and between toruli linear, weakly concave. Mandibles spiniform, tapering to their unidentate apices, thus appearing wedge-shaped in dorsal view. Labrum deeply notched apically, sides distinctly narrowing apicomediad. Palp formula 6,3; maxillary palp relatively long, exceeding hypostomal margin but not occiput; labial palp short, about one-fourth length of maxillary palp. Prementum elongate, diamond shaped. Stipes without transverse carina. Medial hypostomal lamina absent. Pronotum short, strap-like. Mesoscutum relatively long, with maximum length greater than maximum width; notauli absent; parapsides diverging anteriorly; scutoscutellar sulcus distinctly broad; lateral mesopectal sulcus sinuate. Upper metapleural region distinct, about 4 × as long as broad; lower metapleural region indistinct. Propodeum without

distinct dorsal and posterior surfaces; propodeal spiracle small, circular, set slightly below metaphragmal pit. Femora puny, thin; metafemur and metatibia slightly sinuate. Tibial spur formula 1,1. Arolia small, barely visible. Petiole elliptical in lateral view, with broadly convex tergum and sternum; node not squamiform. Abdominal tergum III with broad but shallow concavity anteriorly above helcium. Abdominal segments III–VII similar in size, unmodified. Abdominal sterna VII–VIII broadly emarginate posteriorly. Abdominal sternum IX posterior margin convex, simple. Cerci not visible. Cupula not visible. Gonocoxite length uncertain; gonocoxital apex distinctly offset from gonostylar base. Gonostylus elongate, triangular; length about 2–3 × width; apex narrowly pointed. Volsellae incompletely visible; basivolsellar process present, acute; cuspis absent; lateropenite (= digitus) apex directed ventrad at nearly right angle relative to body of volsella; dorsal margin of digitus almost lobate; digital apices narrowing, almost rod-like and curved laterad. Ventral margins of penites more-or-less linear from base to apex; dorsal margins broadly convex in lateral view; apical processes directed posterad and relatively short, length from proximodorsal inflection point ~ 1 × height. Fore and hind wing venation virtually identical to *R. miafina*. Jugal lobe absent.

**Measurements and indices:** Dashes indicate metric could not be taken or calculated. Holotype: BL ~ 2.34, HL 0.54, HW 0.41, HWE 0.50, EL 0.21, MSL 0.09, FcW –, SL –, OLL –, OIL –, WL 0.91, ML 0.43, MW –, FWL 2.17, PL –, PW 0.09, PH 0.12, GL 0.86, GW 0.43, CI 92, HWI 122, MSI 6, SI –, OI 39, EPI –, OCI –, MI –, PI –. Paratype: BL ~ 2.57, HL 0.54, HW 0.41, HWE 0.48, MSL 0.09, EL 0.22, FcW 0.12, SL 0.22, OLL 0.04, OIL 0.011, WL 0.98, ML 0.46, MW 0.37, FWL 2.52, PL 0.12, PW –, PH 0.15, GL 0.93, GW 0.54, CI 90, HWI –, MSI 6, SI –, OI 40, EPI –, OCI 38, MI 80, PI 80.

**Note:** For comparison, see the metrics for *R. miafina* provided below.

#### *RAVAVY MIAFINA FISHER, 2009*

**Measurements and indices:** ( $N = 4$ , taken from CASENT0078664, CASENT0080308, CASENT0115570, CASENT0474633.) BL c. 3.33–4.46, HL 2.37–2.45, HW 1.84–1.91, HWE 2.13–2.25, EL 0.34–0.43, MSL 0.08–0.09, FcW 0.49–0.55, SL 0.074–0.98, OLL 0.24–0.28, OIL 0.44–0.56, WL 1.30–1.67, ML 0.68–0.78, MW 0.81–0.92, FWL 3.85–4.24, PL 0.15–0.19, PW –, PH 0.28–0.31, GL 1.64–2.29, GW 0.58–0.70, CI 88–92, HWI 112–114 (122), MSI 28–32,



SI 39–53, OI 14–18, EPI –, OCI 44–62, MI 104–129, PI 51–67.

## DISCUSSION

The fossil record of Dolichoderinae spans the Cenozoic to the Late Cretaceous, with ~16% of the total species-level diversity of the subfamily represented by extinct taxa (Bolton, 2022). Of the 137 valid extinct dolichoderine species, 48 are attributed to 20 extinct genera and the remainder are distributed among extant genera of the Dolichoderini (*Dolichoderus* †50 spp.), Leptomyrmecini (*Gracilidris* †1 sp., *Iridomyrmex* Mayr, 1862 †5 spp., *Leptomyrmex* †1 sp.), and Tapinomini (*Liometopum* Mayr, 1861 †20 spp., *Tapinoma* Förster, 1850 †6 spp., *Technomyrmex* †4 spp.). *Ravavy goldmani* is only the second described species of the genus and also constitutes the first fossil member of Bothriomyrmecini. Based on the enhanced application of SR-μ-CT (Figs 1, 2), *Technomyrmex svojtkai* expands the knowledge of this genus.

The genus *Ravavy* was recently established to accommodate a series of males collected in Madagascar, all attributed to a single species, *R. miafina* (Fisher, 2009; Yoshimura & Fisher, 2011). Although they remain undescribed, workers were associated with the male by the Ant Tree of Life research group. Based on this association, it has been found by the myrmecological community that *Ravavy* probably comprises multiple species and is distributed throughout the Afrotropics, including the Democratic Republic of Congo, Ghana, Mozambique, South Africa, Tanzania and Zambia (see data on AntWeb, 2022). As the new records are based almost entirely on workers, plus a dealate queen, the documentation of morphological diversity for male *Ravavy* remains limited to specimens identified as *R. miafina*. The diversity of Malagasy *Ravavy* is certainly underappreciated as well, as a second morphospecies is also known. In any case, the new species described above, *R. goldmani*, represents the first male of the genus recorded from continental Africa, and it shares a suite of derived traits with *R. miafina*, in addition to displaying the diagnostic features of Dolichoderinae and Bothriomyrmecini. Although these species are superficially similar, detailed examination revealed 15 discretized trait differences between the two, as listed in part IV of the diagnosis, thus indicating some degree of phylogenetic distance. The lack of identified male *Loweriella* – the sister-group of *Ravavy* (Ward *et al.*, 2010) – unfortunately complicates the interpretation of generic boundaries. Because *Ravavy* males of other extant morphospecies have yet to be recorded, we cannot provide further discussion on the specific relationship of the fossil to modern lineages.

*Technomyrmex* comprises 94 living species primarily distributed in the Afrotropical, Indomalayan and Australian bioregions (Bolton, 2022). Two species, *T. fulvus* (Wheeler, 1934) and *T. gorgona* Fernández & Guerrero, 2008, are endemic to the Neotropics (Fernández & Guerrero, 2008). Besides an unsubstantiated report of *Technomyrmex* from Canadian Hat Creek amber (Poinar *et al.*, 1999; see: Ward *et al.*, 2010; Archibald *et al.*, 2018), four extinct species have hitherto been attributed to the genus: *T. hispaniolae* Wilson, 1985 and *T. caritatis* Brandão *et al.*, 1999 from Miocene Dominican amber; *T. septentrionalis* Zhang, 1989 from Miocene imprints of Shanwang, China; and *T. deletus* Emery, 1891 from Sicilian amber. While the generic identities of the first three species have been questioned (Bolton, 2007; Fernández & Guerrero, 2008), the placement of *T. deletus* is considered more certain due to preservation and exposure of its proventriculus (Bolton, 2007). The Sicilian and Ethiopian amber species are thus the only definite fossil species of *Technomyrmex*, with *T. deletus* previously hypothesized to have affinity with the *T. albipes* group (Bolton, 2007) and *T. svojtkai* here assumed to be related to the *T. bicolor* group. It is worth noting that the age of Sicilian amber is controversial, being from Late Eocene, Oligocene or Middle Miocene (14–34 Mya; Ragazzi & Roghi, 2014).

The overall morphological similarity of *T. svojtkai* and *R. goldmani* to extant species provides further information about the timing and pattern of ant diversification. The ages of these fossils are congruent with the divergence-dating estimates of Ward *et al.* (2010) for the *Ravavy* + *Loweriella* and *Technomyrmex* crown clades, with suggested age ranges of ~17–42 Mya and ~18–33 Mya, respectively. The Miocene species described here are readily attributable to *Technomyrmex* and *Ravavy* based on a suite of synapomorphies. Indeed, it is possible that *T. svojtkai* and *R. goldmani* are members of the crown clades of their respective genera given that *Technomyrmex* was represented by only three terminals in Ward *et al.* (2010) and the undescribed Afrotropical morphospecies of *Ravavy* were not sampled in that study. Whereas Eocene to Oligocene amber deposits include a mixture of extant and extinct genera plus stem-group species (e.g. Barden, 2017; Boudinot *et al.*, 2022), Miocene deposits are dominated by modern genera and crown-group species (e.g. Barden, 2017; Barden *et al.*, 2017; Prebus, 2017). With the direct fossil record and divergence-time estimates (for summary of the latter, see: Borowiec *et al.*, 2021), the larger pattern emerging across ants is the diversification of clades attributable to extant subfamilies during the Late Cretaceous, to extant genera in the Palaeogene and to modern species since the Mio-Pliocene.

Finally, we provide further corroborating evidence for a Miocene age of Ethiopian amber (Bouju & Perrichot,

2020; Bouju, 2021) via the high abundance and species composition of ants among the total arthropod inclusions. We have examined 84 fossiliferous amber pieces from four collections housed in the NIGPAS, IGR, MAIG and NHMW collections. This material yielded 193 ant individuals (105 males, 85 workers and three alate females), representing six subfamilies and at least 19 genera, as summarized in Table 1. Importantly, the examined material comprised two unbiased samples of 17 and 43 fossiliferous pieces ('IGR' and 'MAIG' samples, respectively) obtained directly from the market at Addis Ababa and purchased without

pre-selection for particular insect or plant taxa. The ant prevalence reaches 48% of total insects in the IGR sample and 52% in the MAIG sample; these values are congruent only with Neogene fossil insect deposits, such as the Miocene Dominican or Mexican amber (LaPolla *et al.*, 2013; Barden, 2017). Further, within the ants, the prevalence of Myrmicinae (75% of all ants in the IGR sample, 54% in the MAIG sample) also supports a Miocene age (Barden, 2017). In contrast, the subfamily Dolichoderinae studied herein is infrequent, accounting for less than 4% of the total ant assemblage examined. We will report on the species identities and

**Table 1.** Diversity and specimen count of ants known from Ethiopian amber (aq, alate queen; m, male; w, worker; acronyms of collections are explained in Material and methods)

Taxa	Number of specimens and castes in each collection			
	IGR	MAIG	NIGPAS	NHMW
<b>Dolichoderinae</b>				
Bothriomyrmecini				
<i>Ravavy</i> Fisher, 2009	1m		1m	
Tapinomini				
<i>Technomyrmex</i> Mayr, 1872		4w		1w
<b>Dorylinae</b>				
gen. indet.		1w		
<b>Formicinae</b>				
Plagiolepidini				
<i>Anoplolepis</i> Santschi, 1914	1w			
<b>Myrmicinae</b>				
Attini				
<i>Pheidole</i> Westwood, 1839	1w			
Crematogastrini				
<i>Cardiocondyla</i> Emery, 1869b		1w		
<i>Carebara</i> Westwood, 1840	5m	2m, 1w	5m	
<i>Cataulacus</i> Smith, 1853		1w		
<i>Melissotarsus</i> Emery, 1877	3w	4w	1m, 1w	
<i>Rhopalomastix</i> Forel, 1900			1aq, 1w	
<i>Trichomyrmex</i> Mayr, 1865	3m, 37w		1m, 2w	
gen. indet.			1m	
Solenopsidini				
<i>Monomorium</i> Mayr, 1855	11w	1m, 1w	1m	
Tribe incertae sedis				
gen. indet.	3m, 1w	2aq, 32m, 5w	1w	
<b>Ponerinae</b>				
Ponerini				
<i>Cryptopone</i> Emery, 1893		6m	1m	
<i>Hypoponera</i> Santschi, 1938		1m	1m	
<i>Euponera</i> ? Forel, 1891	2m			
gen. indet.	3m	13m, 1w	2m	
<b>Pseudomyrmecinae</b>				
<i>Tetraoponera</i> Smith, 1852				1w
<b>Subfamily incertae sedis</b>				
gen. indet.	2m, 3w	17m, 2w		
	TOTAL, ANTS: 193			

morphological diversity of further Ethiopian amber ants in future taxonomic treatments.

## ACKNOWLEDGEMENTS

We warmly thank Matthias Svojtka (University of Vienna), Yale Goldman (Bloomfield, Connecticut) and Marcin Buzalski (Gdansk) for facilitating access to various specimens described or reported here. We are grateful to Amde Zewdalem (Jacksonville, Florida) and Binyam Teferi (Addis Ababa) for information and access to the amber deposits of the North Shewa Zone, Ethiopia; the Ethiopian Ministry of Mines and Petroleum for delivering the export permits; Valentine Bouju and Cédric Chény (Univ. Rennes) for contributing data and preparation of ants from Ethiopian amber; Alexander Schmidt (University of Göttingen) for invaluable discussions, advices and contribution regarding the study of Ethiopian amber; Paul Tafforeau and Carmen Soriano (ESRF) for the exquisite synchrotron imaging of specimen NHMW-N6976; and Bo Wang (NIGPAS) for acquisition and provision of the male specimens described here. We thank Hans Pohl (Friedrich Schiller University Jena) for allowing use of his imaging station. Finally, we thank the editor and anonymous reviewers for their comments. This research was supported by the Alexander von Humboldt Foundation via Research Fellowships to VP (2006–2008) and BEB (2020–2022), Harvard Ernst Mayr travel grants (BEB), the Tellus-INTERRVIE program CNRS INSU (project AMBRAFRICA to VP), the Strategic Priority Research Program of the Chinese Academy of Sciences (XDB26000000), the National Natural Science Foundation of China (42125201, 41688103) and the ESRF through attribution of inhouse beamtime on the beamline ID19.

## CONFLICT OF INTEREST

The authors declare no competing interests.

## DATA AVAILABILITY

The published article includes all morphometric data generated and analyzed during this study. Further information and requests for resources should be directed to the lead contact, Vincent Perrichot ([vincent.perrichot@univ-rennes1.fr](mailto:vincent.perrichot@univ-rennes1.fr)).

## REFERENCES

**AntWeb. 2022.** *AntWeb v.8.68.7*. Berkeley: California Academy of Sciences. Available at: <https://www.antweb.org> (accessed 7 January 2022).

- Archibald SB, Cover SP, Moreau CS. 2006.** Bulldog ants of the Eocene Okanagan Highlands and history of the subfamily (Hymenoptera: Formicidae: Myrmecinae). *Annals of the Entomological Society of America* **99**: 487–523.
- Archibald SB, Rasnitsyn AP, Brothers DJ, Mathewes RW. 2018.** Modernisation of the Hymenoptera: ants, bees, wasps, and sawflies of the early Eocene Okanagan Highlands of western North America. *The Canadian Entomologist* **150**: 205–257.
- Barden P. 2017.** Fossil ants (Hymenoptera: Formicidae): ancient diversity and the rise of modern lineages. *Myrmecological News* **24**: 1–30.
- Barden P, Boudinot BE, Lucky A. 2017.** Where fossils dare and males matter: combined morphological and molecular analysis untangles the evolutionary history of the spider ant genus *Leptomyrmex* Mayr (Hymenoptera: Dolichoderinae). *Invertebrate Systematics* **31**: 765–780.
- Bolton B. 1994.** *Identification guide to the ant genera of the world*. Cambridge: Harvard University Press.
- Bolton B. 2003.** Synopsis and classification of Formicidae. *Memoirs of the American Entomological Institute* **71**: 1–370.
- Bolton B. 2007.** Taxonomy of the dolichoderine ant genus *Technomyrmex* Mayr (Hymenoptera: Formicidae) based on the worker cast. *Contributions of the American Entomological Institute* **35**: 1–150.
- Bolton B. 2022.** *An online catalogue of the ants of the world*. Available at: <http://www.antcat.org> (accessed 7 January 2022)
- Borowiec ML, Moreau CS, Rabeling C. 2021.** Ants: phylogeny and classification. In: Starr C, ed. *Encyclopedia of social insects*. Cham: Springer International Publishing, 52–69.
- Boudinot BE. 2013.** The male genitalia of ants: musculature, homology, and functional morphology (Hymenoptera, Aculeata, Formicidae). *Journal of Hymenoptera Research* **30**: 29–49.
- Boudinot BE. 2015.** Contributions to the knowledge of Formicidae (Hymenoptera, Aculeata): a new diagnosis of the family, the first global male-based key to subfamilies, and a treatment of early branching lineages. *European Journal of Taxonomy* **120**: 1–62.
- Boudinot BE. 2018.** A general theory of genital homologies for the Hexapoda (Pancrustacea) derived from skeletomuscular correspondences, with emphasis on the Endopterygota. *Arthropod Structure & Development* **47**: 563–613.
- Boudinot BE, Probst RS, Brandão CRF, Feitosa RM, Ward PS. 2016.** Out of the Neotropics: newly discovered relictual species sheds light on the biogeographical history of spider ants (*Leptomyrmex*, Dolichoderinae, Formicidae). *Systematic Entomology* **41**: 658–671.
- Boudinot BE, Moosdorf OTD, Beutel RG, Richter A. 2021.** Anatomy and evolution of the head of *Dorylus helvolus* (Formicidae: Dorylinae): patterns of sex- and caste-limited traits in the sausagefly and the driver ant. *Journal of Morphology* **282**: 1616–1658.
- Boudinot BE, Borowiec ML, Prebus MM. 2022.** Phylogeny, evolution, and classification of the ant genus *Lasius*, the tribe Lasiini, and the subfamily Formicinae (Hymenoptera: Formicinae). *Systematic Entomology* **47**: 113–151.



- Bouju V. 2021.** *Paléobiodiversité et paléoenvironnements des gisements à ambre du Crétacé et du Miocène d'Afrique*. Unpublished Ph. D. Thesis, Université de Rennes 1.
- Bouju V, Perrichot V. 2020.** A review of amber and copal occurrences in Africa and their paleontological significance. *BSGF-Earth Sciences Bulletin* **191**: 17.
- Bouju V, Rosse-Guillevic S, Griffon M, Bojarski B, Szwedo J, Perrichot V. 2021.** The genus *Allodia* (Diptera: Mycetophilidae) in Miocene Ethiopian amber. *Fossil Record* **24**: 339–346.
- Bouju V, Feldberg K, Kaasalainen U, Schäfer-Verwimp A, Hedenäs L, Buck WR, Wang B, Perrichot V, Schmidt AR. 2022a.** Miocene Ethiopian amber: a new source of fossil cryptogams. *Journal of Systematics and Evolution*. doi: [10.1111/jse.12796](https://doi.org/10.1111/jse.12796).
- Bouju V, Jouault C, Perrichot V. 2022b.** The termite genus *Glyptotermes* (Isoptera: Kalotermitidae) in Miocene amber from Ethiopia. *Journal of Paleontology* **96**: 387–393.
- Brandão CRF, Baroni Urbani C, Wagensberg J, Yamamoto C. 1999.** ('1998'). New *Technomyrmex* in Dominican amber (Hymenoptera: Formicidae), with a reappraisal of Dolichoderinae phylogeny. *Entomologica Scandinavica* **29**: 411–428.
- Coty D, Lebon M, Nel A. 2016.** When phylogeny meets geology and chemistry: doubts on the dating of Ethiopian amber. *Annales de la Société Entomologique de France* **52**: 161–166.
- Dlussky GM, Brothers DJ, Rasnitsyn AP. 2004.** The first Late Cretaceous ants (Hymenoptera: Formicidae) from southern Africa, with comments on the origin of the Myrmicinae. *Insect Systematics and Evolution* **35**: 1–13.
- Dubovikoff DA. 2005.** The system of taxon *Bothriomyrmex* Emery, 1869 sensu lato (Hymenoptera: Formicidae) and relatives genera. *Caucasian Entomological Bulletin* **1**: 89–94 [in Russian].
- Emery C. 1869a.** Descrizione di una nuova formica italiana. *Annuario del Museo Zoologico della Reale Università di Napoli* **5**: 117–118.
- Emery C. 1869b.** Enumerazione dei formicidi che rinvenngonsi nei contorni di Napoli con descrizioni di specie nuove o meno conosciute. *Annali dell'Accademia degli Aspiranti Naturalisti. Secunda Era* **2**: 1–26.
- Emery C. 1877.** Catalogo delle formiche esistenti nelle collezioni del Museo Civico di Genova. Parte prima. Formiche provenienti dal Viaggio dei signori Antinori, Beccari e Issel nel Mar Rosso e nel paese dei Bogos. [concl.]. *Annali del Museo Civico di Storia Naturale* **9**: 369–381.
- Emery C. 1891.** Le formiche dell' ambra Siciliana nel Museo Mineralogico dell'Università di Bologna. *Memorie della Reale Accademia delle Scienze dell'Istituto di Bologna* **5**: 141–165 [pagination of separate 568–591], pls 1–3.
- Emery C. 1893 ('1892').** [Untitled. Introduced by: 'M. C. Emery, de Bologne, envoie les diagnoses de cinq nouveaux genres de Formicides']. *Bulletin Bimensuel de la Société Entomologique de France* **1892**: 275–277.
- Emery C. 1913 ('1912').** Hymenoptera. Fam. Formicidae. Subfam. Dolichoderinae. *Genera Insectorum* **137**: 1–50.
- Fernández F, Guerrero RJ. 2008.** *Technomyrmex* (Formicidae: Dolichoderinae) in the New World: synopsis and description of a new species. *Revista Colombiana de Entomología* **34**: 110–115.
- Fisher BL. 2009.** Two new dolichoderine ant genera from Madagascar: *Aptinoma* gen. n. and *Ravavy* gen. n. (Hymenoptera: Formicidae). *Zootaxa* **2118**: 37–52.
- Fisher BL, Bolton B. 2016.** *Ants of Africa and Madagascar: a guide to the genera*. Berkeley: University of California Press.
- Forel A. 1878.** Études myrmécologiques en 1878 (première partie) avec l'anatomie du gésier des fourmis. *Bulletin de la Société Vaudoise des Sciences Naturelles* **15**: 337–392.
- Forel A. 1891.** Les Formicides. [part]. In: Grandidier A, ed. *Histoire physique, naturelle, et politique de Madagascar. Vol. XX. Histoire naturelle des Hyménoptères. Deuxième partie (28e fascicule)*. Paris: Hachette et Cie.
- Forel A. 1900.** Un nouveau genre et une nouvelle espèce de Myrmicide. *Annales de la Société Entomologique de Belgique* **44**: 24–26.
- Förster A. 1850.** *Hymenopterologische Studien. 1. Formicariae*. Aachen: Ernst Ter Meer.
- Harris RA. 1979.** A glossary of surface sculpturing. *Occasional Papers in Entomology. State of California Department of Food and Agriculture* **28**: 1–31.
- Harrison T, Msuya CP, Murray AM, Jacobs BF, Báez AM, Mundil R, Ludwig KR. 2001.** Paleontological investigations at the Eocene locality of Mahenge in North-Central Tanzania, East Africa. In: Gunnell GF, ed. *Eocene biodiversity: unusual occurrences and rarely sampled habitats*. Boston: Springer. *Topics in Geobiology* **18**: 39–74.
- Keller RA. 2011.** A phylogenetic analysis of ant morphology (Hymenoptera: Formicidae) with special reference to the poneromorph subfamilies. *Bulletin of the American Museum of Natural History* **355**: 1–90.
- Lak M, Néraudeau D, Nel A, Cloetens P, Perrichot V, Tafforeau P. 2008.** Phase contrast X-ray synchrotron imaging: opening access to fossil inclusions in opaque amber. *Microscopy and Microanalysis* **14**: 251–259.
- LaPolla JS, Dlussky GM, Perrichot V. 2013.** Ants and the fossil record. *Annual Reviews of Entomology* **58**: 609–630.
- Latreille PA. 1809.** *Genera crustaceorum et Insectorum secundum ordinem naturalem in familias disposita, iconibus exemplisque plurimis explicata. Tomus 4*. Paris and Strasbourg: A. Koenig.
- Lucky A, Ward PS. 2010.** Taxonomic revision of the ant genus *Leptomyrmex* Mayr (Hymenoptera: Formicidae). *Zootaxa* **2688**: 1–67.
- Lund PW. 1831.** Lettre sur les habitudes de quelques fourmis du Brésil, adressée à M. Audouin. *Annales des Sciences Naturelles* **23**: 113–138.
- Mayr G. 1855.** Formicina austriaca. Beschreibung der bisher im österreichischen Kaiserstaate aufgefundenen Ameisen, nebst Hinzufügung jener in Deutschland, in der Schweiz und in Italien vorkommenden Arten. *Verhandlungen der Zoologisch-Botanischen Vereins in Wien* **5**: 273–478.
- Mayr G. 1861.** *Die europäischen Formiciden. Nach der analytischen Methode bearbeitet*. Wien: C. Gerolds Sohn.
- Mayr G. 1862.** Myrmecologische Studien. *Verhandlungen der Kaiserlich-Königlichen Zoologisch-Botanischen Gesellschaft in Wien* **12**: 649–776.

- Mayr G. 1865.** Formicidae. In: *Novara Expedition 1865. Reise der Österreichischen Fregatte 'Novara' um die Erde in den Jahren 1857, 1858, 1859. Zoologischer Theil. Bd. II. Abt. 1.* Wien: K. Gerold's Sohn.
- Mayr G. 1872.** Formicidae Borneensis collectae a J. Doria et O. Beccari in territorio Sarawak annis 1865–1867. *Annali del Museo Civico di Storia Naturale* **2**: 133–155.
- Mikó I, Trietsch C, Sandall EL, Yoder MJ, Hines H, Deans AR. 2016.** Malagasy *Conostigmus* (Hymenoptera: Ceraphronoidea) and the secret of scutes. *PeerJ* **4**: e2682.
- Perrichot V, Boudinot BE, Cole J, Delhay-Prat V, Esnault J, Goldman Y, Nohra YA, Schmidt AR. 2016.** African fossiliferous amber: a review. In: Penney D, Ross AJ, eds. *Abstracts of the 7th international conference on fossil insects, arthropods, and amber, held in Edinburgh, Scotland, in April–May 2016.* Manchester: Siri Scientific Press, 41.
- Perrichot V, Boudinot BE, Chény C, Cole J, Jeanneau L, Schmidt A, Szwedo J, Wang B. 2018.** The age and paleobiota of Ethiopian amber revisited. *5th International Palaeontological Congress, held in Paris, France, in July 2018.* Abstract book, 23.
- Petrunkévitch AI. 1955.** Arachnida. In: Moore RC, ed. *Treatise on invertebrate palaeontology, Part P. Arthropoda 2.* Lawrence: Geological Society of America & University of Kansas Press, 42–162.
- Poinar G Jr, Archibald B, Brown A. 1999.** New amber deposit provides evidence of early Paleogene extinctions, paleoclimates, and past distributions. *The Canadian Entomologist* **131**: 171–177.
- Prebus MM. 2017.** Insights into the evolution, biogeography and natural history of the acorn ants, genus *Temnothorax* Mayr (Hymenoptera: Formicidae). *BMC Evolutionary Biology* **17**: 250.
- Ragazzi E, Roghi G. 2014.** Simetite, the Sicilian amber. In: Kustatscher E, Roghi G, Bertini A, Miola A, eds. *Palaeobotany of Italy. Publication of the Museum of Nature South Tyrol* **9**: 232–237.
- Richter A, Hita Garcia F, Keller RA, Billen J, Economu EP, Beutel, RG. 2020.** Comparative analysis of worker head anatomy of *Formica* and *Brachyponera* (Hymenoptera: Formicidae). *Arthropod Systematics & Phylogeny* **78**: 122–170.
- Sadowski EM, Schmidt AR, Seyfullah LJ, Solórzano-Kraemer MM, Neumann C, Perrichot V, Hamann C, Milke R, Nascimbene PC. 2021.** Conservation, preparation and imaging of diverse ambers and their inclusions. *Earth-Science Reviews* **220**: 103653.
- Santschi F. 1914.** Voyage de Ch. Alluaud et R. Jeannel en Afrique Orientale, 1911–1912. *Résultats scientifiques. Insectes Hyménoptères. II. Formicidae.* Paris: Libr. A. Schulz.
- Santschi F. 1919.** Fourmis du genre *Bothriomyrmex* Emery (Systématique et mœurs). *Revue Zoologique Africaine* **7**: 201–224.
- Santschi F. 1938.** Notes sur quelques *Ponera* Latr. *Bulletin de la Société Entomologique de France* **43**: 78–80.
- Schlüter T. 2018.** Eocene insects from a Maar Lagerstätte at Mahenge, northern Tanzania. *Entomologia Generalis* **37**: 375–392.
- Schmidt AR, Perrichot V, Svojtka M, Anderson KB, Belet KH, Bussert R, Dörfelt H, Jancke S, Mohr B, Mohrmann E, Nascimbene PC, Nel A, Nel P, Ragazzi E, Roghi, G., Saupe EE, Schmidt K, Schneider H, Selden PA, Vávra N. 2010.** Cretaceous African life captured in amber. *Proceedings of the National Academy of Sciences of the USA* **107**: 7329–7334.
- Shattuck SO. 1992.** Generic revision of the ant subfamily Dolichoderinae (Hymenoptera: Formicidae). *Sociobiology* **21**: 1–181.
- Smith F. 1852.** Descriptions of some hymenopterous insects captured in India, with notes on their economy, by Ezra T. Downes, Esq., who presented them to the Honourable the East India Company. *Annals and Magazine of Natural History* **9**: 44–50.
- Smith F. 1853 ('1854').** Monograph of the genus *Cryptocerus*, belonging to the group *Cryptoceridae* – family *Myrmicidae* – division *Hymenoptera Heterogyna*. *Transactions of the Entomological Society of London* **2**: 213–228.
- Smith F. 1860.** Catalogue of hymenopterous insects collected by Mr. A. R. Wallace in the islands of Bachian, Kaisaa, Amboyna, Gilolo, and at Dory in New Guinea. *Journal and Proceedings of the Linnean Society of London. Zoology* **5(Suppl. to vol. 4)**: 93–143.
- Solórzano-Kraemer MM, Hammel JU, Kunz R, Xu C, Cognato AI. 2022.** Miocene pinhole borer ambrosia beetles: new species of *Diapys* (Coleoptera: Curculionidae: Platypodinae). *Palaeoworld* **31**. Doi: [10.1016/j.palwor.2021.10.001](https://doi.org/10.1016/j.palwor.2021.10.001).
- Szadziewski R, Sontag E, Pankowski MV. 2021.** A new biting midge of the genus *Forcipomyia* Meigen, 1818 from Miocene Ethiopian amber (Diptera: Ceratopogonidae). *Palaeontology* **4**: 441–444.
- Ulitzka MR. 2020.** Two fossil thrips from Ethiopian amber (Thysanoptera) with description of *Merothrips aithiopicus* sp. n. (Thysanoptera: Merothripidae). *Zootaxa* **4786**: 283–288.
- Ward PS, Brady SG, Fisher BL, Schultz TR. 2010.** Phylogeny and biogeography of dolichoderine ants: effects of data partitioning and relict taxa on historical inference. *Systematic Biology* **59**: 342–362.
- Westwood JO. 1839.** *An introduction to the modern classification of insects; founded on the natural habits and corresponding organisation of the different families. Vol. 2, Part XI.* London: Longman, Orme, Brown, Green and Longmans.
- Westwood JO. 1840.** Observations on the genus *Typhlopone*, with descriptions of several exotic species of ants. *Annals and Magazine of Natural History* **6**: 81–89.
- Wheeler WM. 1934.** Neotropical ants collected by Dr. Elisabeth Skwarra and others. *Bulletin of the Museum of Comparative Zoology at Harvard College* **77**: 160–240.
- Wild AL, Cuzzo F. 2006.** Rediscovery of a fossil dolichoderine ant lineage (Hymenoptera: Formicidae: Dolichoderinae) and a description of a new genus from South America. *Zootaxa* **1142**: 57–68.
- Wilson EO. 1985.** Ants of the Dominican amber (Hymenoptera: Formicidae). 3. The subfamily Dolichoderinae. *Psyche* **92**: 17–37.
- Wilson EO, Taylor RW. 1964.** A fossil ant colony: new evidence of social antiquity. *Psyche* **71**: 93–103.

- Wunderlich J. 2017.** Description of a derived spider taxon in Ethiopian amber (Araneae: Salticidae). *Beiträge zur Araneologie* **10**: 280–284.
- Yoshimura M, Fisher BL. 2011.** A revision of male ants of the Malagasy region (Hymenoptera: Formicidae): key to genera of the subfamily Dolichoderinae. *Zootaxa* **2794**: 1–34.
- Yoshimura M, Fisher BL. 2012.** A revision of male ants of the Malagasy Amblyoponinae (Hymenoptera: Formicidae) with resurrections of the genera *Stigmatomma* and *Xymmer*. *PLoS One* **7**: e33325.
- Zhang J. 1989.** *Fossil insects from Shanwang, Shandong, China*. Jinan, China: Shandong Science and Technology Publishing House [in Chinese, with English summary].

## SUPPORTING INFORMATION

Additional Supporting Information may be found in the online version of this article at the publisher's website.

**Figure S1.** Animated 3D volume rendering of *Technomyrmex svojtkai*, holotype worker NHMW-N6976.

**Figure S2.** Animated 3D volume rendering of *Technomyrmex svojtkai*, holotype worker NHMW-N6976. Body view with legs removed.

**Appendix S1.** Measurement file and values for males of *Ravavy* species.